Aqueous Chemical Growth of α-Fe_2O_3–α-Cr_2O_3 Nanocomposite Thin Films

Lionel Vayssieres,* Jinghua Guo, and Joseph Nordgren

Department of Physics, Uppsala University, Box 530, SE-75121 Uppsala, Sweden

We are reporting here on the inexpensive fabrication and optical properties of an iron(III) oxide–chromium(III) oxide nanocomposite thin film of corundum crystal structure. Its novel and unique-designed architecture consists of uniformed, well-defined and oriented nanorods of Hematite (α-Fe_2O_3) of 50 nm in diameter and 500 nm in length and homogeneously distributed nonaggregated monodisperse spherical nanoparticles of Eskolaite (α-Cr_2O_3) of 250 nm in diameter. This α-Fe_2O_3–α-Cr_2O_3 nanocomposite thin film is obtained by growing, directly onto transparent polycrystalline conducting substrate, an oriented layer of hematite nanorods and growing subsequently, the eskolaite layer. The synthesis is carried out by a template-free, low-temperature, multilayer thin film coating process using aqueous solution of metal salts as precursors. Almost 100% of the light is absorbed by the composite film between 300 and 525 nm and 40% at 800 nm which yields great expectations as photoanode materials for photovoltaic cells and photocatalytic devices.

Keywords: Eskolaite, Hematite, Iron oxide, Chromium Oxide, Nanocomposite, Nanorod, Thin Film, Aqueous Processing, Photoanode, Optical Properties.

COMMUNICATION

Nanocomposite materials (i.e., consisting of more than one nanophase) have been extensively studied over the last decades and have been engineered from homogeneous ceramics to thin film coatings for nanotechnology, and industrial applications of such novel and functional materials are impending. An important topic of the research and development of nanocomposite materials is the crucial industrial, economical, and environmental issue of corrosion[1] and corrosion resistance of metals and alloys. Indeed, extended fundamental knowledge is required to understand the relation between morphology, crystallinity and composition of the compounds involved in the oxidation and passivity of metals and alloys[2] in industrial applications such as metallurgy and hydrometallurgy.

Iron–chromium oxide composites are important materials in corrosion science and have been under scrutiny to study artificial passivation[3] of stainless steel and binary alloys and their thin film dissolution processes.[4] Indeed, the combination of these two oxides is of importance for the fundamental understanding of corrosion reactions, corrosion resistance, and metal passivity[5] as well as model system to probe and demonstrate the general relation between structure, crystallinity, and composition on the corrosion properties of transition metal oxide composite thin films.[6] Indeed, the corrosion resistance in acidic medium of Fe–Cr composite oxide films has been shown to depend on the content of Cr in doped α-Fe_2O_3 (hematite) or of α-Cr_2O_3 (eskolaite) content or both in the composite film. The Cr^{3+} ion is reported as very efficient inhibitor of hematite dissolution.[7]

Besides the corrosion science studies, such composite materials are extensively studied for their surface and catalytic properties,[8,9] like for instance the oxidation of CO by O_2. In addition, photoelectrochemical applications of iron oxides and its mixed and composite materials are of importance for the creation of novel and more efficient anodes for photocatalytic[10] and photovoltaic devices.[11] Indeed, improving the optical absorption properties as well as electronic conductivity of such materials will represent a significant step for the quest of stable, reliable, and cheap materials for sustainable renewable catalytic systems as well as for energy conversion and storage applications. Indeed, a significant improvement of the light absorption profile and photoelectrochemical properties is expected due to combination of the *red* hematite and the *green* eskolaite. The synthesis of a black Fe_2O_3–Cr_2O_3 ceramic pigment has recently been reported.[12]

Accordingly, developing novel physical and chemical synthesis processing to design nanocomposite transition metal oxide materials is of importance for fundamental and applied research and of relevance for industrial applications. Hitherto, the synthesis of the Fe–Cr composite oxide thin films was typically conducted in vacuum by sputtering technique,[3,5,13,14] and by metallorganic chemical vapor deposition (MOCVD) on hot substrates from acetylacetonate precursors.[6,15]

The purpose of this communication is to demonstrate the ability to generate large arrays of well-designed

*Author to whom correspondence should be addressed.

  1533-4880/2001/04/385/004/$17.00+.25 doi:10.1166/jnn.2001.055

α-Fe_2O_3–α-Cr_2O_3 nanocomposite thin film materials on polycrystalline transparent conducting oxide (TCO) substrate or single crystalline sapphire at low cost, by a controlled aqueous low-temperature thin film growth process. Our synthetic approach to shape-up materials and create novel and functional (purpose-built) devices is based on a concept[16] and an aqueous chemical growth processing technique sustained by a thermodynamic model of nucleation, growth, and aging control via the minimization of the interfacial tension of the system.[17,18] Such aqueous thin film growth processing method is applicable to produce metal oxide thin films on various substrates with more complex architecture for enhanced efficiency, and novel or improved properties in view of creating a new generation of smart and functional nanomaterials at low costs.[16] Such approach has been already successfully applied to the design of large three-dimensional arrays of crystalline and highly oriented hematite nanorods as well as multiband-gap thin films.[19] Their orientation and the unique structural design[20] where the nanorods diameter is matching the minority carrier diffusion length resulted in an incident photon-to-electron conversion efficiency (IPCE) of 60% at 350 nm which led to the development of the first iron oxide, sandwich-type, wet photovoltaic cell.[21] In addition, three-dimensional highly oriented hexagonal microrod-array of zincite ZnO[22] have been obtained on various types of substrates showing high photoefficiency and excellent electron transport properties in the UV range as studied by laser transient spectroscopy. Recently, large arrays of aligned and highly oriented ZnO microtubes[23] have also been successfully produced by following the same concept and solution thin film processing technique to demonstrate the ability to create, at low cost, large arrays of well-ordered and highly porous microparticulate thin film materials for instance for chemical, gas, and biosensors applications.

The thermodynamically stable crystal structure of chromium(III) oxide and of iron(III) oxide is corundum and occurs in nature as the mineral Eskolaite[24] and Hematite,[25] respectively. These sesquioxides (M_2O_3) crystallize in the rhombohedral (trigonal–hexagonal) crystal system, space group $R\bar{3}c \equiv D^6_{3d}$, and they are isostructural with α-Al_2O_3 (corundum), and V_2O_3 (karelianite). The lattice is built on a hexagonal close-packed (HCP) array of oxygen with four of every six available octahedral sites around O atoms occupied with the cation. The octahedral and tetrahedral sites are above and below one another in a HCP lattice, the tetrahedral sites remaining empty. Octahedra are sharing faces along a threefold axis and are distorted to trigonal antiprisms because of the cation–cation repulsion occurring across one shared face and not the others. This yields to very dense and very hard covalent structures with a high oxygen packing index, resulting in strongly colored materials of high polarizability and high refractive index.

The synthesis procedure consists in growing the well-ordered and oriented iron oxide nanorod layer onto transparent conducting polycrystalline (or single crystalline) substrates to study its optical and photoelectrochemical properties. Subsequently, the chromium oxide layer is grown onto the iron oxide layer to create the designed nanocomposite thin film materials.

The growth of the three-dimensional array of crystalline highly oriented hematite nanorod bundles was conducted according to Ref. 19. The synthesis was performed with reagent grade chemicals. An aqueous solution (MilliQ, 18.2 MΩcm) of 0.15 M of ferric chloride ($FeCl_3 \cdot 6H_2O$) and 1 M of sodium nitrate ($NaNO_3$) at pH 1.5 (set by HCl) mixed in a glass bottle with autoclavable screw cap (e.g., Duran laboratory) containing a polycrystalline TCO substrate (e.g., F–SnO_2 Hartford Glass Inc.) or a single-crystalline Al_2O_3 substrate (sapphire) was heated in a laboratory oven at a constant temperature of 95 °C for 24 h. Subsequently, the durable and scratch resistant thin films are thoroughly washed with water to remove any residual salts. A heat-treatment in air at 450 °C for 1 h is performed to obtain the pure thermodynamically stable crystallographic phase of ferric oxide (i.e., hematite).

The synthesis consists of creating the nanocomposite materials by heteroepitaxial growth of the corundum α-Cr_2O_3 layer directly onto the corundum α-Fe_2O_3 nanorod array. Whereas the two minerals are isomorphic, heteronucleation is energetically more favorable (low-activation energy barrier) than homogenous nucleation. The interfacial energy between the two solids is smaller than the interfacial energy between the crystals and the solution, and therefore heteronucleation of the chromium layer is promoted and may take place at a lower saturation ratio onto the iron oxide layer rather than in solution. The same synthetic technique as previously described for the hematite layer was used. A glass bottle with polypropylene (PP) screw cap containing thin films of hematite nanorod-array on TCO (or sapphire) and a 1 mM aqueous solution (MilliQ) of chromium alum, $KCr(SO_4)_2 \cdot 12H_2O$, is heated at a constant temperature of 85 °C in a laboratory oven for 24 h allowing for the hydrolysis-condensation process of the $[Cr(H_2O)_6]^{3+}$ ion and its subsequent nucleation and growth process as eskolaite onto the hematite thin film to occur. Afterwards, the thin films are thoroughly washed with (MilliQ) water to remove any residual salts. Subsequently, the thin films are heat-treated at a constant temperature of 500 °C in an oven for 1 h to obtain the stoichiometric and thermodynamically stable corundum composite nanomaterials consisting of Hematite and Eskolaite. The film thickness is typically of 0.7 μm as determined by profilometry (Tencor Alpha Step).

Figure 1 shows the field-emission gun scanning electron micrographs (LEO 1530 Gemini FEG-SEM) of the nanocomposite material at various magnifications. Monodisperse and nonaggregated spherical mesoparticles

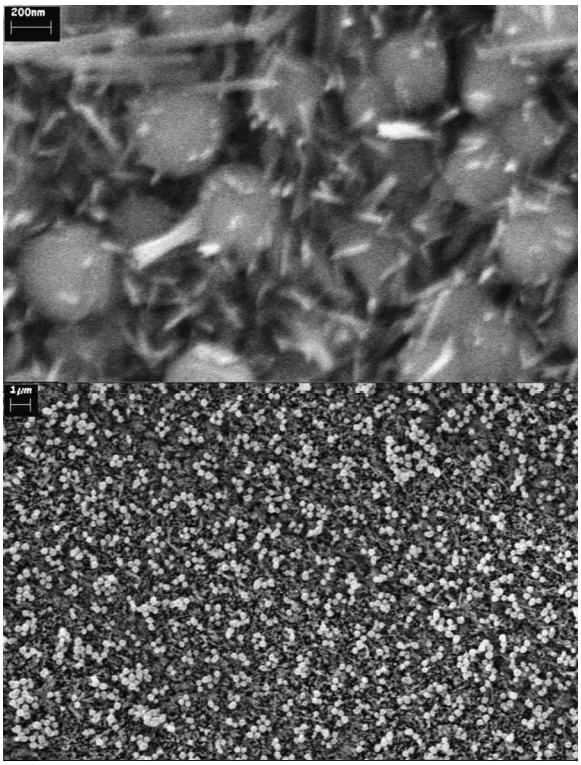

Fig. 1. Field-emission gun scanning electron micrographs (FEG–SEM) of the α-Fe_2O_3–α-Cr_2O_3 nanocomposite thin film consisted of hematite-oriented nanorods and eskolaite spherical mesoparticles.

of Eskolaite of 250 nm in diameter are homogeneously distributed in the oriented array of hematite nanorod bundles of 50 nm in diameter (consisting of nanorods of 3 nm in diameter[19,20]) and about 500 nm in length. Full coverage of several tens of centimeter square scratch resistant thin films (and potentially much larger with larger substrate and container) is easily produced. A strong adhesion of the chromium layer onto the iron layer is obtained as well as the iron oxide layer onto the substrate because the thin films are grown from molecular precursors directly onto the substrate. In addition, the isostructural property (corundum crystal structure) between the two transition metal oxides contributes to the overall mechanical stability of the nanocomposite.

The X-ray diffraction (XRD) pattern of a 700 nm thick α-Fe_2O_3–α-Cr_2O_3 nanocomposite thin film grown onto conducting F–SnO_2 glass substrate was recorded on a Siemens D-5000 diffractometer (Bragg–Brentano focusing geometry). The pattern shows that the nanocomposite is crystalline and the corundum structures of hematite and eskolaite (Fig. 2) are clearly identified as well as the diffraction peak of the substrate (fluorine-doped tin oxide). The position of the diffraction peaks and corresponding miller indices are found in accordance to JCPDS 38-1479 for eskolaite and 33-0664 for hematite.

The optical characterization of the nanocomposite thin films was carried out in the UV-visible range on a 5240

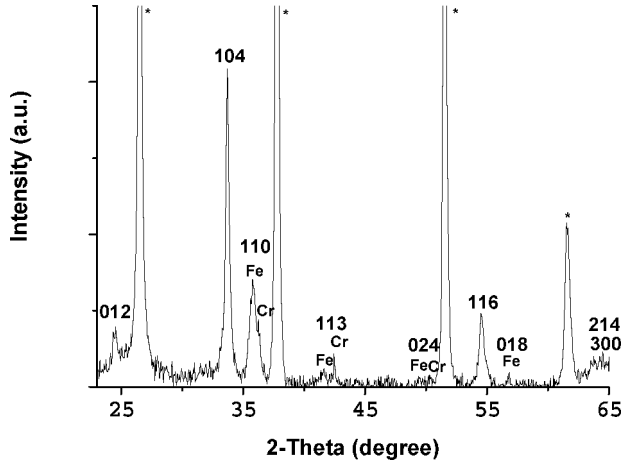

Fig. 2. Indexed XRD pattern (Cu K_α) of a 0.7 μm corundum α-Fe_2O_3–α-Cr_2O_3 nanocomposite thin film recorded at a step of 0.05° (2θ) and 60 s per step. The $*$ symbol denotes the substrate diffraction peaks (F–SnO_2).

Beckman spectrophotometer equipped with an integrated sphere. All measurements were performed on dry films, in air and at room temperature. A tungsten lamp was used as light source with a grating monochromator and a photomultiplier detector. The optical data were recorded at a scan speed of 2 nm per second and were corrected from substrate effect. The data were processed according to Ref. 26. The absorptance A was calculated according to the following equation $A = 1 - R - T$, where R and T are the total (diffuse + specular) reflectance and transmittance, respectively (Fig. 3). The translucent brown thin films showed a very strong absorptance, very close to 1 (100% of the light absorbed), in the range 300–525 nm followed by a monotone linear decrease to 0.5 at 650 nm. The absorptance slowly declined to 0.4 at 800 nm (40% of the light absorbed) and did not reach zero, most probably

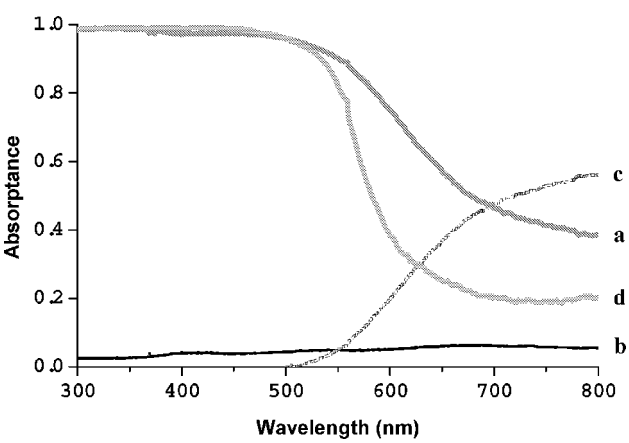

Fig. 3. UV-visible optical characteristics: (a) absorptance, (b) total reflectance, (c) total transmittance spectra of the α-Fe_2O_3–α-Cr_2O_3 nanocomposite thin film and (d) absorptance spectrum of α-Fe_2O_3 nanorod thin film; grown on transparent conducting glass substrate.

originating from multiple absorption phenomena within the nanocomposite film or scattering at the film/substrate interface. The total reflectance of the thin films remained at a very low level (5%) within the whole range of wavelength investigated revealing very low amount of light scattering of the film.

As expected, the absorptance spectrum of the α-Fe_2O_3–α-Cr_2O_3 nanocomposite is found to be significantly red-shifted compared to bare α-Fe_2O_3 thin films due to the broad absorption (centered at 570 nm) of the α-Cr_2O_3 layer due to the d–d transitions from the d^3 ion Cr^{3+} in octahedral symmetry ($^4A_{2g} \rightarrow {}^4T_{2g}$). The absorption profile of the composite film covers to a great extent the visible solar spectrum yielding great expectations as photoanode materials for photoelectrochemical applications such as photovoltaic cells, water splitting and photocatalytic devices.

The in-depth study of the electronic structure of such nanocomposite is currently under scrutiny at synchrotron facilities by soft X-ray absorption and emission spectroscopies (XAS, XES) and its fine structure is investigated by XANES/EXAFS to probe the relation between its structural and electronic and optical properties.

The design and development of other transition (and post-transition) metal oxide (wide band-gap semiconductor, magnetic and metallic conductor) nanocomposite thin film materials and three-dimensional arrays based on ZnO, Fe_3O_4 and RuO_2 is currently under investigation by low-temperature controlled aqueous chemical growth.

References and Notes

1. Corrosion Science, *MRS Bulletin* **24**, 12 (1999).
2. E. McCafferty, *Corros. Sci.* **42**, 1993 (2000).
3. P. Schmuki, S. Virtanen, H. S. Isaacs, M. P. Ryan, A. J. Davenport, H. Böhni, and T. Stenberg, *J. Electrochem. Soc.* **145**, 791 (1998).
4. J. Manjanna, G. Venkateswaran, B. S. Sherigana, and P. V. Nayak, *Hydrometallurgy* **60**, 155 (2001).
5. M. Son, N, Akao, N. Hara, and K. Sugimoto, *J. Electrochem. Soc.* **148**, B43 (2001).
6. H. Kim, N. N. Hara, and K. Sugimoto, *J. Electrochem. Soc.* **146**, 3679 (1999).
7. G. Bondietti, J. Sinniger, and W. Stumm, *Colloids Surfaces A* **79**, 157 (1993).
8. G. A. El-Shobaky, G. A. Fagal, H. G. El-Shobaky, and S. M. El-Khouly, *Colloids Surfaces A* **152**, 275 (1999).
9. G. A. Fagal, G. A. El-Shobaky, and S. M. El-Khouly, *Colloids Surfaces A* **178**, 287 (2001).
10. Y. Matstumoto, *J. Solid State Chem.* **126**, 227 (1996).
11. S. U. M. Khan and J. Akikusa, *J Phys. Chem. B* **103**, 7184 (1999).
12. A. Escardino, S. Mestre, A. Barba, V. Beltran, and A. Blasco, *J. Am. Ceram. Soc.* **83**, 29 (2000).
13. T. Stenberg, J. Keranen, P. Vuoristo, T. Mantyla, S. Virtanen, P. Schmuki, M. Buchler, and H Bohni, *Vaccum* **52**, 477 (1999).
14. T. Kosaka, S. Suzuki, M. Saito, Y. Waseda, E. Matsubara, K. Sadamori, and E. Aoyagi, *Thin Solid Films* **289**, 74 (1996).
15. K. Sugimoto, M. Seto, S. Tanaka, and N. Hara, *J. Electrochem. Soc.* **140**, 1586 (1993).
16. L. Vayssieres, A. Hagfeldt, and S.-E. Lindquist, *Pure Appl. Chem.* **72**, 47 (2000).
17. L. Vayssieres, Ph.D. Dissertation, Université Pierre et Marie Curie, Paris (1995).
18. L. Vayssieres, C. Chaneac, E. Tronc, and J. P. Jolivet, *J. Colloid Interface Sci.* **205**, 205 (1998).
19. L. Vayssieres, N. Beermann, S.-E. Lindquist, and A. Hagfeldt, *Chem. Mater.* **13**, 233 (2001).
20. L. Vayssieres, J.-H. Guo, and J. Nordgren, *Mater. Res. Soc. Symp. Proc.* **635**, C781 (2001).
21. N. Beermann, L. Vayssieres, S.-E. Lindquist, and A. Hagfeldt, *J. Electrochem. Soc.* **147**, 2456 (2000).
22. L. Vayssieres, K. Keis, S.-E. Lindquist, and A. Hagfeldt, *J. Phys. Chem. B* **105**, 3350 (2001).
23. L. Vayssieres, K. Keis, A. Hagfeldt, and S.-E. Lindquist, accepted for publication to *Chem. Mater*.
24. O. Kouvo and Y. Vuorelainen, *Am. Miner.* **43**, 1098 (1958).
25. L. Pauling and S. B. Hendricks, *J. Am. Chem. Soc.* **47**, 781 (1925).
26. A. Roos, *Sol. Energy Mater. Sol Cells* **30**, 77 (1993); *Appl. Opt.* **30**, 468 (1991).

Received: 30 June 2001. Revised/Accepted: 25 August 2001.